

Superconductivity in the 2D Hubbard model: Electron doping is different

D. Eichenberger and D. Baeriswyl

Department of Physics, University of Fribourg, CH-1700 Fribourg, Switzerland.

(Dated: September 15, 2021)

A variational Monte Carlo calculation is used for studying the ground state of the two-dimensional Hubbard model, including hopping between both nearest and next-nearest neighbor sites. Superconductivity with d -wave symmetry is found to be restricted to densities where the Fermi surface crosses the magnetic zone boundary. The condensate energy is much larger for hole doping than for electron doping. Superconductivity is kinetic energy driven for hole doping, but potential energy driven for electron doping. Our findings agree surprisingly well with experimental data for layered cuprates, both for electron- and hole-doped materials.

PACS numbers: 71.10.Fd, 74.20.Mn, 74.72.-h

It is widely accepted that the layered cuprates are doped Mott insulators, which are well described by the two-dimensional Hubbard model, at least regarding the insulating antiferromagnetic state of the parent compounds and the transition to a metallic state upon doping. Whether this model embodies superconductivity has been debated since two decades, but recent results obtained with improved numerical techniques strengthen the case of pairing induced by on-site repulsion. Progress has been made both in dynamical mean-field theory [1, 2], where an effective attraction is deduced from the irreducible two-particle vertex, and in variational calculations [3, 4], where a broken-symmetry ground state with a d -wave superconducting order parameter is found in a certain density range and for large enough values of U .

The Hubbard Hamiltonian $\hat{H} = \hat{H}_0 + U\hat{D}$ consists of a hopping term (“kinetic energy”)

$$\hat{H}_0 = - \sum_{i,j,\sigma} t_{ij} (c_{i\sigma}^\dagger c_{j\sigma} + c_{j\sigma}^\dagger c_{i\sigma}) \quad (1)$$

and an on-site repulsion $U\hat{D}$, where $\hat{D} = \sum_i n_{i\uparrow} n_{i\downarrow}$ is the number of doubly occupied sites, $n_{i\sigma} = c_{i\sigma}^\dagger c_{i\sigma}$, and the operator $c_{i\sigma}^\dagger$ ($c_{i\sigma}$) creates (annihilates) an electron at site i with spin σ .

In our previous work [4] we have restricted ourselves to nearest-neighbor hopping ($t_{ij} = t$ for nearest-neighbor sites, 0 otherwise). We have used the variational ansatz

$$|\Psi\rangle = e^{h\hat{H}_0/t} e^{-g\hat{D}} |\Psi_0\rangle, \quad (2)$$

which yields a substantial improvement with respect to the Gutzwiller wave function ($h = 0$), and comes very close to the exact ground state both for small 2D systems [5] and for the solvable 1/r chain [6]. Both antiferromagnetic and superconducting states have been chosen as mean-field states $|\Psi_0\rangle$. Antiferromagnetism was found to prevail at half filling, while d -wave pairing has been obtained for the doped system, below a hole concentration of 0.18. At first sight these results seem to contradict recent work by Aimi and Imada [7], who see no signature for superconductivity in their Monte Carlo simulation.

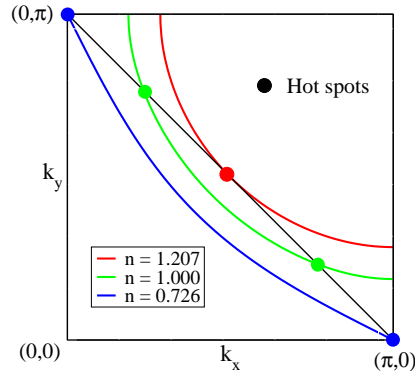


FIG. 1: (Color online) Fermi surface for three different electron densities.

A closer examination shows that there is no discrepancy. On the one hand, the hole densities considered by Aimi and Imada for up to 10x10 lattices (0.18, 0.22, 0.28) are in a region where we obtained a vanishing superconducting order parameter [4]. On the other hand, for the only other density studied by Aimi and Imada (0.09) their result is inconclusive. In fact, for their parameter values ($U/t=6$, lattice size 8x8) the order parameter is expected to be too small to lead to a contradiction [3].

With hopping restricted to nearest-neighbor sites the Hubbard Hamiltonian (on the square lattice) is electron-hole symmetric and there is no difference between electron and hole doping. However, this restriction leads to a (bare) Fermi surface which disagrees qualitatively with photoemission experiments on layered cuprates [8]. In the present paper we investigate the more realistic case where hopping between both nearest (t) and next-nearest neighbors (t') is included. We use parameters $U = 8t$ and $t' = -0.3t$ throughout. The bare single-particle spectrum

$$\epsilon_{\vec{k}} = -2t(\cos k_x + \cos k_y) - 4t' \cos k_x \cos k_y$$

leads to the Fermi surfaces of Fig. 1. The innermost line corresponds to the van Hove filling where the Fermi surface passes through the saddle points at $(\pi, 0)$ and $(0, \pi)$. These crossings between the Fermi surface and the mag-

n	μ	g	h	E/t
0.7500	-0.9921(1)	4.2(1)	0.113(2)	-0.858(1)
0.7800	-0.9612(3)	4.0(1)	0.112(2)	-0.829(1)
0.8125	-0.9107(3)	3.9(1)	0.111(2)	-0.795(1)
0.8400	-0.788(1)	3.7(1)	0.111(2)	-0.763(1)
0.9000	-0.728(1)	3.8(1)	0.111(2)	-0.676(1)
0.9500	-0.603(1)	4.0(1)	0.114(2)	-0.591(1)

TABLE I: Chemical potential, parameters g and h and energy per site for hole doping ($n < 1$) and an 8×8 lattice.

n	μ	g	h	E/t
1.0500	0.7666(1)	3.6(1)	0.109(2)	-0.222(1)
1.0800	0.6440(1)	3.4(1)	0.106(2)	-0.069(1)
1.1000	0.5488(1)	3.2(1)	0.104(2)	0.040(1)
1.1300	0.4380(1)	3.0(1)	0.100(2)	0.206(1)
1.1600	0.3870(1)	2.9(2)	0.096(3)	0.374(1)
1.2000	-0.2996(1)	2.6(2)	0.091(3)	0.608(1)

TABLE II: Chemical potential, parameters g and h and energy per site for electron doping ($n > 1$) and an 8×8 lattice.

netic zone boundary (the “hot spots”) move inwards as the density n is increased and finally merge (outermost line). Hot spots are restricted to $0.726 < n < 1.206$. Our results, to be discussed below, indicate that superconductivity occurs only in this range.

Here we use again the variational ansatz of Eq. (1), but restrict ourselves on a d -wave superconducting ground state, which introduces, in addition to g and h , two other parameters, the amplitude Δ of the superconducting gap function and the “chemical potential” μ . To compute the variational energy, the exponent of the operator $e^{-g\hat{D}}$ is first decoupled by applying a discrete Hubbard-Stratonovich transformation [9], which introduces an Ising spin at each site. All operators are then quadratic in creation and annihilation operators and therefore the fermionic degrees of freedom can be integrated out. The remaining sum over Ising spin configurations is performed by a Monte Carlo simulation. In order to avoid the minus sign problem, calculations are carried out in the grand canonical ensemble with an average density fixed by μ , which is therefore not a variational parameter. To reduce the statistical error, the optimization procedure is based on the method proposed by Ceperley *et al.* [10, 11]. We have used periodic-antiperiodic boundary conditions.

The minimization of the energy E for fixed average densities yields the results of Tables I and II for hole and electron doping, respectively. We notice that the parameter g , which controls the crossover between itinerant (small g) and “localized” (large g) many-particle states, remains large for hole doping, but decreases rapidly for electron doping. Therefore, while the hole-doped region $0.75 < n < 0.95$ is a “localized” doped Mott insulator,

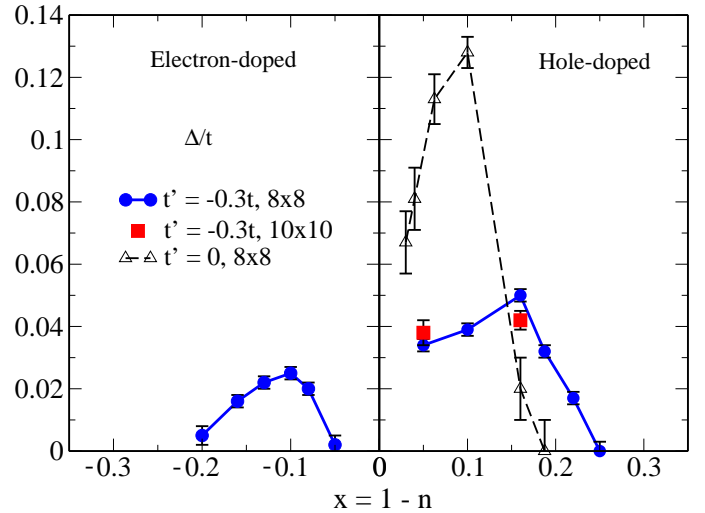


FIG. 2: (Color online) Optimized gap parameter as a function of doping for two different lattice sizes. For comparison, the result for $t' = 0$ is also shown (from Ref. [4]).

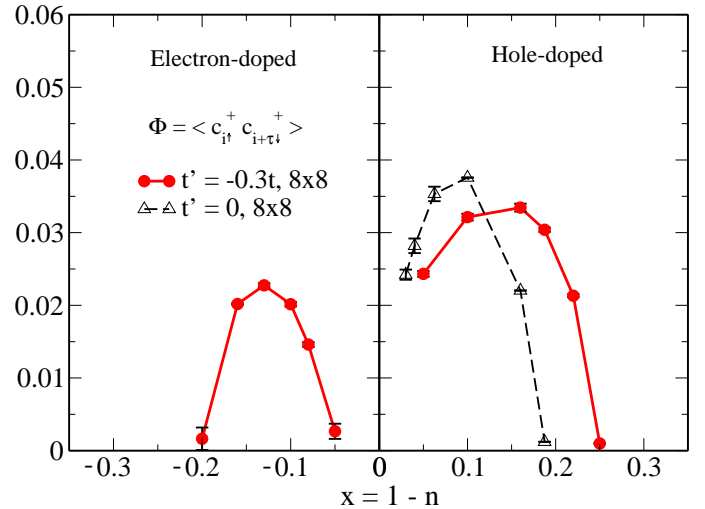


FIG. 3: (Color online) Superconducting order parameter as a function of doping for an 8×8 lattice.

the electron-doped part $1.05 < n < 1.2$ rapidly undergoes a crossover to an itinerant regime as n increases. We attribute this difference to the bare single-particle density of states at the Fermi energy, which is much larger for hole than for electron doping.

Figs. 2 and 3 show, respectively, the gap parameter Δ and the superconducting order parameter $\Phi = |\langle c_{i\uparrow}^\dagger c_{j\downarrow}^\dagger \rangle|$ as functions of doping concentration $x = 1 - n$. The corresponding results for $t' = 0$ [4] are completely electron-hole symmetric and reproduced only in the right panels. On the hole-doped side superconductivity exists for $0 < x < 0.25$ (Δ remains finite, but Φ vanishes for $x \rightarrow 0$), *i.e.* in a larger region than for $t' = 0$. In contrast, on the electron-doped side the superconducting region is reduced to $-0.2 < x < -0.05$. Thus we

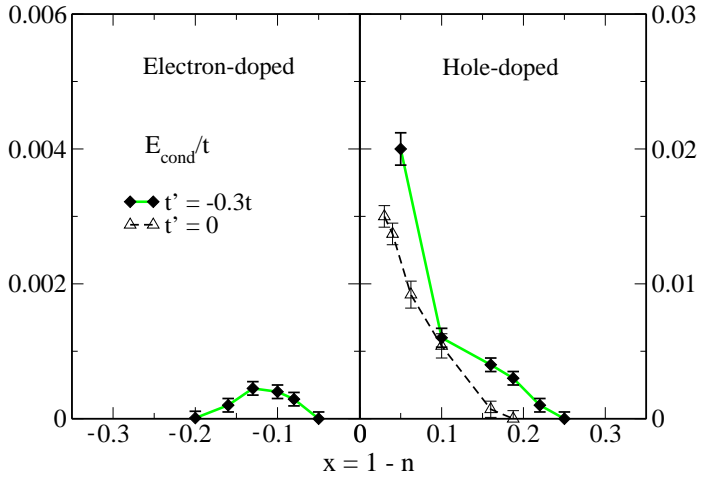


FIG. 4: (Color online) Condensation energy per site for an 8×8 lattice.

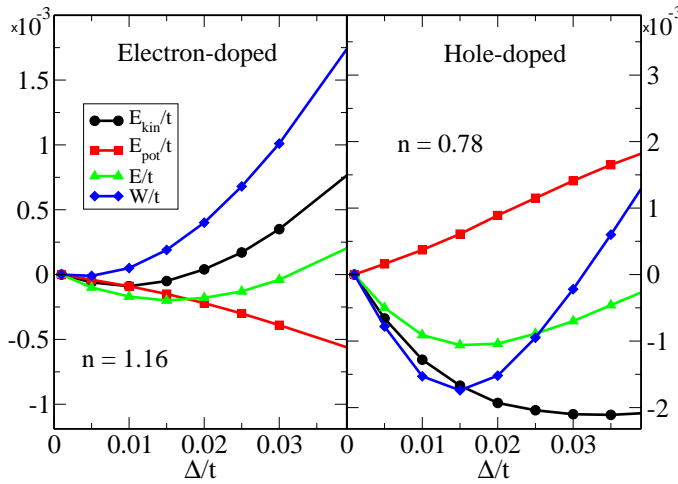


FIG. 5: (Color online) Changes in kinetic, potential and total energies as well as in the quantity W as functions of the gap parameter, for an 8×8 lattice. ($-W$ is proportional to the oscillator strength for intraband transitions.) The relative uncertainties are smaller than the symbol sizes.

find indeed that superconductivity is restricted to densities where the (bare) Fermi surface passes through hot spots (see Fig. 1). The qualitative difference between electron- and hole-doping for $x \rightarrow 0$ suggests that superconductivity competes strongly with antiferromagnetic order (which we did not take into account in this study) on the hole-doped side and weakly on the electron-doped side. Further support for this conclusion comes from the condensation energy $E_{cond} = E(0) - E(\Delta)$, which is one order of magnitude smaller for electron doping than for hole doping, as depicted in Fig. 4.

Fig. 5 shows the kinetic, potential and total energies as functions of the gap parameter for the two densities $n = 0.78$ and 1.16 . For hole doping the energy gain is clearly due to a decrease in kinetic energy, while for

electron doping the decrease in potential energy gives the main contribution to the condensation energy. The same behavior has been consistently obtained for other densities. The quantity

$$W = -2 \sum_{\vec{k}} \frac{\partial^2 \epsilon_{\vec{k}}}{\partial k_x^2} \langle n_{\vec{k}} \rangle, \quad (3)$$

also plotted in Fig. 5, is – up to a minus sign – proportional to the integrated optical conductivity originating from intraband transitions [12]. For the simple Hubbard model ($t' = 0$) W is equal to the kinetic energy, but for $t' \neq 0$ the two quantities differ. For hole doping W has a pronounced minimum in the region of the optimal gap, corresponding to an increase of oscillator strength, while for electron doping W increases monotonically with Δ , akin to BCS behavior where the oscillator strength is reduced at the onset of superconductivity.

We attribute this asymmetry between hole and electron doping to the different values of the correlation parameter g (see Tables I and II), which puts the hole-doped system into the “localized” regime, while the electron-doped system is more itinerant. To make the point clear we consider the simple Hubbard model ($t' = 0$) both in the small U (itinerant) and large U (“localized”) limits. In the small U limit superconductivity is produced by the Kohn-Luttinger mechanism [13], where the condensation energy is expected to increase as a function of U/t , whereas in the large U limit the condensation energy arises from magnetic exchange and thus is likely to increase with t/U . The change in kinetic energy is then obtained through the Hellman-Feynman theorem,

$$E_{kin}(\Delta) - E_{kin}(0) = -t \frac{\partial}{\partial t} E_{cond}, \quad (4)$$

which is positive in the small U limit and negative in the large U limit.

Additional information can be gained from the magnetic structure factor

$$S(\vec{q}) = \frac{1}{N} \sum_{i,j} e^{i\vec{q} \cdot (\vec{R}_i - \vec{R}_j)} \langle (n_{i\uparrow} - n_{i\downarrow})(n_{j\uparrow} - n_{j\downarrow}) \rangle, \quad (5)$$

displayed in Fig. 6. $S(\vec{q})$ exhibits a clear maximum at (π, π) , which is largest close to half filling and decreases as doping increases. There is very little difference between electron and hole doping, presumably because in the large U limit spin correlations depend mostly through the exchange constants $J = 4t^2/U$ and $J' = 4t'^2/U$ on the microscopic parameters and therefore are essentially independent on the sign of t' .

We have seen above that superconductivity is restricted to the region where two points of the Fermi surface can be connected (at least approximately) by the antiferromagnetic wave vector (π, π) . This together with the strong peak of $S(\vec{q})$ for $\vec{q} = (\pi, \pi)$ supports

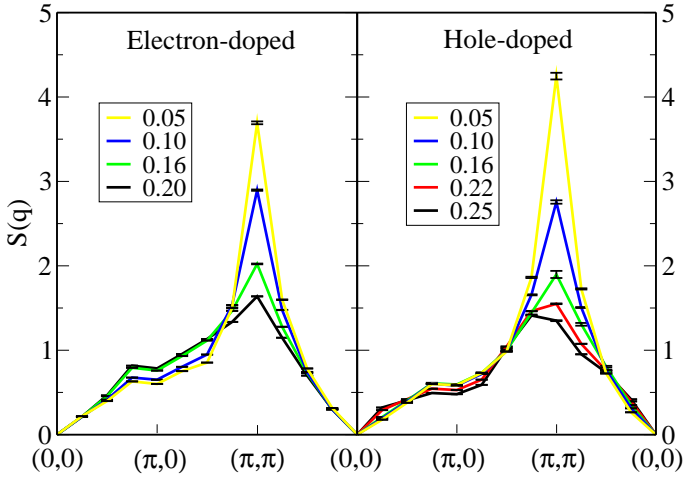


FIG. 6: (Color online) Magnetic structure factor as a function of the momentum, for various densities above and below half filling, for an 8×8 lattice.

the point of view that superconductivity in the two-dimensional Hubbard model is due to a magnetic mechanism. This conclusion is now widely accepted, but the question whether the mechanism is of the RVB type [14] or arises from the exchange of spin fluctuations [15] is presently under debate [16, 17]. We cannot solve this problem on the basis of our variational calculations, but the distinction between “localized” and itinerant regimes can give additional useful insight. According to our results the former is appropriate for the hole-doped region, where superconductivity is associated with a decrease in kinetic energy, the latter regime is found for electron doping, where superconductivity arises from a more conventional gain in potential energy.

The results described above compare surprisingly well with experiments on cuprates, better than our earlier calculations [4] where only nearest neighbor hopping has been taken into account. This concerns the phase diagram, in particular for electron-doped materials for which a recent systematic study [18] gives a dome-shape (for T_c) strikingly similar to our Fig. 2. Photoemission data give values of the superconducting gap Δ in the range 10-20 meV for hole-doped compounds (LSCO [19] or Bi2201 [8]) and ~ 5 meV for an electron-doped compound (Nd-CeCO [20]). Choosing $t = 300$ meV (neutron data), our maximum gap parameters are 15 and 7 meV for hole and electron doping, respectively. An increase of oscillator strength, predicted by our calculations for hole doping, has been reported on the basis of optical spectroscopy for an underdoped sample [21], but the situation is less clear on the overdoped side. We are not aware of corresponding measurements on electron-doped materials.

In conclusion, our variational search for d -wave superconductivity in the two-dimensional Hubbard model gives a differentiated picture, namely a large (moderate) correlation parameter for hole (electron) doping, a gain

in kinetic (potential) energy due to pairing and a large (small) condensation energy. Our wave function is expected to be better suited for describing the electron-doped region, which is less “localized” than the hole-doped region. More work is needed to improve our understanding of the pseudogap phase observed in the cuprates for weak hole doping, by studying possible competing instabilities.

We are grateful for financial support from the Swiss National Science Foundation through the National Center of Competence in Research “Materials with Novel Electronic Properties-MaNEP”. The computations have been partially performed on the Pléiades cluster of the EPFL.

- [1] T. A. Maier, M. Jarrell, and D. J. Scalapino, Phys. Rev. B **74**, 094513 (2006).
- [2] K. Haule and G. Kotliar, Phys. Rev. B **76**, 104509 (2007).
- [3] H. Yokoyama, Y. Tanaka, M. Ogata, and H. Tsuchiura, J. Phys. Soc. Jpn. **73**, 1119 (2004).
- [4] D. Eichenberger and D. Baeriswyl, Phys. Rev. B **76**, 180504(R) (2007).
- [5] H. Otsuka, J. Phys. Soc. Jpn. **61**, 1645 (1991).
- [6] M. Dzierzawa, D. Baeriswyl, and M. DiStasio, Phys. Rev. B **51**, 1993 (1995).
- [7] T. Aimi and M. Imada, J. Phys. Soc. Jpn. **76**, 113708 (2007).
- [8] A. Damascelli, Z. Hussain, and Z.-X. Shen, Rev. Mod. Phys. **75**, 473 (2003).
- [9] J. E. Hirsch, Phys. Rev. B **28**, 4059 (1983).
- [10] D. Ceperley, G. V. Chester, and K. H. Kalos, Phys. Rev. B **16**, 3081 (1977).
- [11] C. J. Umrigar, K. G. Wilson, and J. W. Wilkins, Phys. Rev. Lett. **60**, 1719 (1988).
- [12] D. Baeriswyl and L. Degiorgi, *Strong Interactions in Low Dimensions*, vol. 25 of *Physics and Chemistry of Materials with Low-Dimensional Structures* (Kluwer Academic Publishers, 2004), especially chapters by A. J. Millis and D. van der Marel.
- [13] W. Kohn and J. M. Luttinger, Phys. Rev. Lett. **15**, 524 (1965).
- [14] P. W. Anderson, Science **235**, 1196 (1987).
- [15] D. Scalapino, J. Low Temp. Phys. **117**, 179 (1999).
- [16] P. W. Anderson, Science **316**, 1705 (2007).
- [17] T. A. Maier, D. Poilblanc, and D. J. Scalapino, Phys. Rev. Lett. **100**, 237001 (2008).
- [18] Y. Krockenberger, J. Kurian, A. Winkler, A. Tsukada, M. Naito, and L. Alff, arXiv:0805.0978.
- [19] K. Yamada, S. Wakimoto, G. Shirane, C. H. Lee, M. A. Kastner, S. Hosoya, M. Greven, Y. Endoh, and R. J. Birgeneau, Phys. Rev. Lett. **75**, 1626 (1995).
- [20] T. Sato, T. Kamiyama, T. Takahashi, K. Kurahashi, and K. Yamada, Science **291**, 1517 (2001).
- [21] F. Carbone, A. B. Kuzmenko, H. J. A. Molegraaf, E. van Heumen, V. Lukovac, F. Marsiglio, D. van der Marel, K. Haule, G. Kotliar, H. Berger, et al., Phys. Rev. B **74**, 064510 (2006).